

RESEARCH ARTICLE OPEN ACCESS

Cryogenian Glacial Erosion and Tectonics as Agents of Crustal Recycling

M. Seraine^{1,2}  | C. J. Spencer¹ | T. M. Gernon^{3,4} | T. Hincks³  | C. L. Kirkland²  | E. Rugen⁵ | L. DaSilva¹  | H. Shafaii Moghadam⁶ | L. P. Soares⁷ | G. Fazio⁸

¹Department of Geological Science and Geological Engineering of Queen's University, Kingston, Ontario, Canada | ²Timescales of Mineral Systems Group, Curtin Frontier Institute of Geoscience Solutions, School of Earth and Planetary Sciences, Curtin University, Perth, Western Australia, Australia | ³School of Ocean and Earth Science, University of Southampton, Southampton, UK | ⁴GFZ Helmholtz Centre for Geosciences, Potsdam, Germany | ⁵Department of Earth Sciences, University College London, London, UK | ⁶Xinjiang Research Centre for Mineral Resources, Xinjiang Institute of Ecology and Geography, Chinese Academy of Sciences, Urumqi, China | ⁷Institute of Astronomy, Geophysics and Atmospheric Sciences (IAG), University of São Paulo, São Paulo, Brazil | ⁸Departamento de Geofísica, Observatório Nacional, Rio de Janeiro, Brazil

Correspondence: M. Seraine (marina.seraine@gmail.com; marina.seraine@curtin.edu.au)

Received: 28 May 2025 | **Revised:** 8 September 2025 | **Accepted:** 19 September 2025

Keywords: crustal evolution | crustal recycling | glacial | neoproterozoic | snowball | statistics

ABSTRACT

Zircon preserves evidence of recycling processes that link surface environments to the mantle. Combined $\delta^{18}\text{O}$ - ϵHf in zircon fingerprints magmatic sources and tracks how crustal material is reworked over time. We apply statistical analyses to a global compilation that apparently resolves shifts in zircon U-Pb, $\delta^{18}\text{O}$, and Lu-Hf data spanning the Neoproterozoic. Between ~750 and 705 Ma, a decline in crustal residence ages suggests recycling of juvenile crust into subduction zones, overlapping with the onset of the Sturtian glaciation and potentially driven by erosion of Tonian basaltic provinces. After 705 Ma, residence ages increase, marking intensified crustal recycling during the Sturtian and Marinoan glaciations, supported by ϵHf and $\delta^{18}\text{O}$ change points at ~690 Ma. This transition towards greater incorporation of ancient sediments may reflect tectonic instability during Rodinia's breakup and glacial erosion. These findings suggest a complex interplay between tectonics, climate, and large igneous province processes in shaping Earth's crustal evolution.

1 | Introduction

The Neoproterozoic (1000–538.8 Ma), which is subdivided into the Tonian, Cryogenian, and Ediacaran periods, has been extensively studied for its records of substantial changes in Earth's tectonic and climatic systems. This includes (a) a state shift increase in oxygen levels in the atmosphere, known as the Neoproterozoic Oxygenation Event (NOE) (Shields-Zhou and Och 2011); (b) episodes of widespread glaciation during the Cryogenian (Hoffman et al. 2017) and younger Ediacaran (Wang et al. 2023); (c) breakup of the Rodinia supercontinent (Li et al. 2023) (Figure 1); (d) evolution of complex multicellular life (Eriksson et al. 2013); and (e) the emplacement of numerous

large igneous provinces (LIPs) (Ernst et al. 2021). Among these, the emplacement of large basaltic provinces between 825 and 755 Ma is suggested as a potential trigger to initiate the Sturtian glaciation (Goddéris et al. 2003). Silicate weathering under tropical conditions is one mechanism that could lead to CO_2 draw-down, ultimately forcing global cooling (Cox et al. 2016).

Two major glacial episodes have been identified at low paleolatitudes in the Neoproterozoic: the Sturtian (ca. 717 Ma to 660 Ma) (Rooney et al. 2020), and the Marinoan (ca. 645 Ma to 635 Ma) (Hoffman et al. 2017; Prave et al. 2016). Kirschvink (1992) proposed the Snowball Earth hypothesis to explain the presence of these low-paleolatitude glacial deposits, suggesting that during

[Correction added on 24 October 2025, after first online publication: The given name of co-author T. Gernon has been updated to T. M. Gernon.]

This is an open access article under the terms of the [Creative Commons Attribution-NonCommercial-NoDerivs](https://creativecommons.org/licenses/by-nc-nd/4.0/) License, which permits use and distribution in any medium, provided the original work is properly cited, the use is non-commercial and no modifications or adaptations are made.

© 2025 The Author(s). *Terra Nova* published by John Wiley & Sons Ltd.

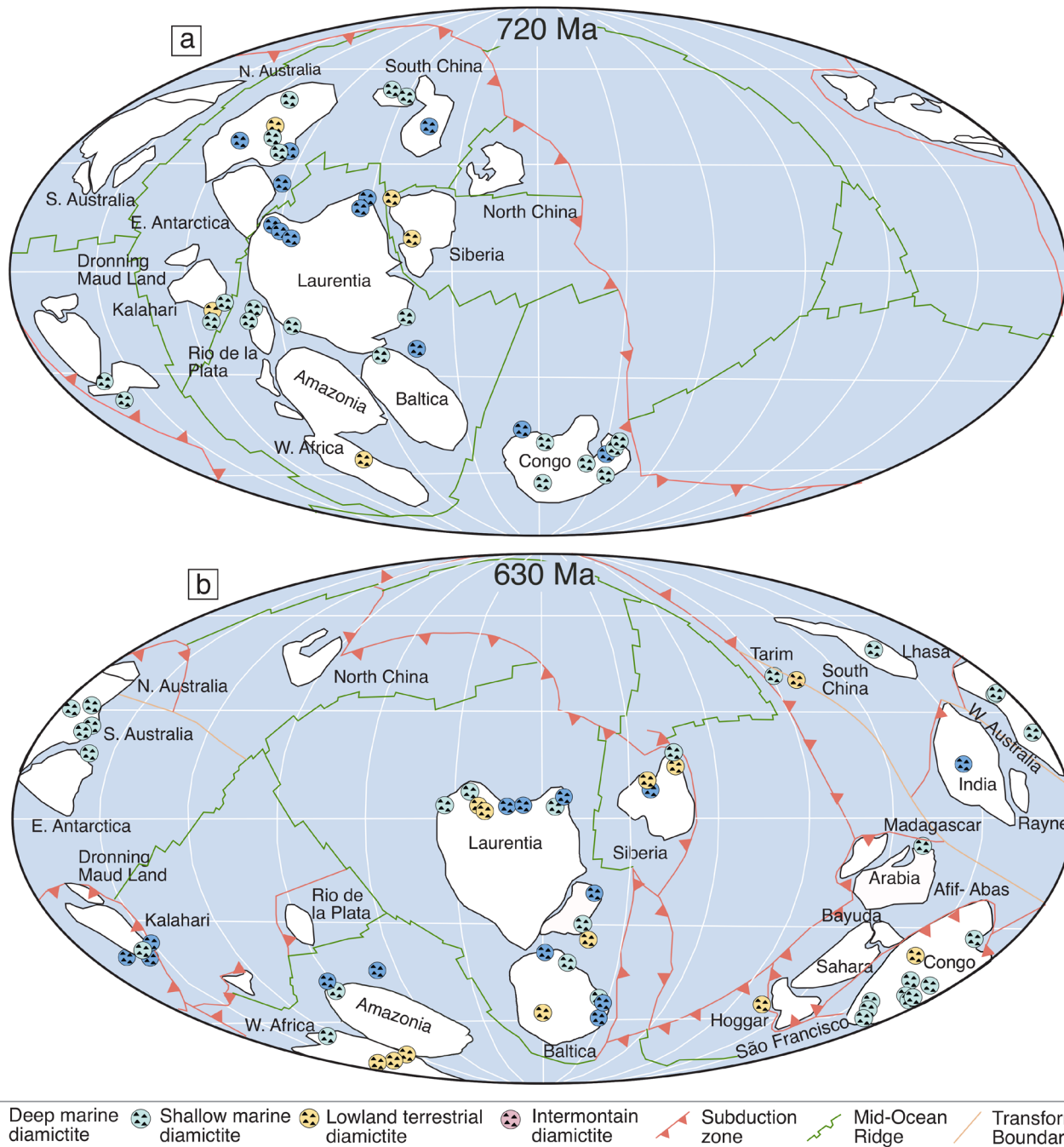


FIGURE 1 | Global plate tectonic reconstruction featuring the continental configuration during the Cryogenian period as well as the glacial facies and tectonic features. Diagrams are modified after Li et al. (2023). [Colour figure can be viewed at [wileyonlinelibrary.com](https://onlinelibrary.wiley.com)]

these events, continental ice cover was thin and patchy, with oceans covered by sea ice and the hydrological cycle essentially stalled. However, other studies have presented sedimentological evidence indicating the existence of an active hydrological cycle during this time, inferring a more “slush ball” planetary state (Allen and Etienne 2008; Christie-Blick et al. 1999).

Glaciations commonly drive high rates of localised erosion (Wilner et al. 2024), as exemplified by modern Norwegian fjords and their Cryogenian counterparts (Mitchell et al. 2019). For the Snowball Earth events, a global average of 3–5 km of glacial erosion has been inferred, potentially accounting for widespread unconformities in the late Proterozoic stratigraphic

record (Keller et al. 2019). Additional evidence for significant Neoproterozoic erosion includes a coincident shift in local sedimentary provenance (Rugen Elias et al. 2024) and thermochronological data from North America that supports substantial Cryogenian exhumation (McDannell et al. 2022).

Despite these observations, the thickness of Cryogenian sedimentary successions (i.e., the products of continental erosion) ostensibly appears to contradict the expectation of high erosion rates during this period. Instead, sedimentological evidence suggests a much slower median accumulation rate, about an order of magnitude lower than that of Phanerozoic glaciations (Partin and Sadler 2016). Additionally, thermochronology suggests that

exhumation did not coincide with glaciation, and this discrepancy has led to alternative explanations for the unconformities observed in the late Proterozoic (Flowers et al. 2020). To clarify the significance of any purported Neoproterozoic erosion event, further testing is required.

Sedimentary materials deposited in ocean basins can be incorporated into magmatic systems during subduction (Plank et al. 2007; Sobolev and Brown 2019). U–Pb geochronology, Lu–Hf, and $\delta^{18}\text{O}$ isotopes in zircon have been used as proxies to understand sediment recycling and ancient tectonic settings. The U–Pb and Lu–Hf isotope systems in zircon crystals provide information about mantle versus crustal sources in magmatic systems, whereas $\delta^{18}\text{O}$ provides insights into the assimilation of different types of rocks and their interaction with the hydrosphere (Bindeman 2008). The reworking of supracrustal materials is often associated with elevated $\delta^{18}\text{O}$ values and low ϵHf signatures, due to the prolonged near-surface history of evolved crust and its remnants (Valley et al. 2005). During the Cryogenian, the correlation between zircon Hf and O isotopes has been interpreted as a paleo-erosion proxy, reflecting glacial erosion and sediment subduction (Keller et al. 2019).

In this study, we compiled coupled U–Pb, Lu–Hf, and O isotopes from 2895 individual magmatic and detrital zircon grains (Puetz et al. 2024) (Table S1; Figures S1 and S2), applied step-change analysis using Conjugate Partitioned Recursion (CPR) and Theil–Sen regression to investigate the intensity of erosion and sediment incorporation into magmatic systems during the Cryogenian glaciation. Locally Estimated Scatterplot Smoothing (LOESS) is applied to crustal residence ages to investigate potential shifts in the material being recycled into magmatic systems through time. In addition, we compiled the temporal frequency of LIP activity and orogenesis (Condie et al. 2022) to evaluate whether multiple processes may influence erosion and magmatic recycling rates, and to investigate the extent to which these possible drivers are integrated.

2 | Results

2.1 | Oxygen Isotopes

We applied a conjugate partitioned recursion (CPR) to a zircon of $\delta^{18}\text{O}$ time series spanning 900 Ma to 500 Ma to investigate potential step changes in oxygen isotopes through time. Change-point models, such as CPR, may indicate a state shift, where the algorithm searches for a location to divide the data with different means. Overall, $\delta^{18}\text{O}$ exhibits significant variation through time, with a bimodal pattern during 850 Ma to 800 Ma, followed by a substantial shift towards mantle-like values between 800 Ma and 720 Ma, defining a cluster around $\sim 5\%$. The change point analysis reveals an increase in $\delta^{18}\text{O}$ values at 682 Ma (Figure 2a), within the Sturtian glaciation.

2.2 | Hf Isotopes

From a broader perspective, the LOESS regression trend shows a gradual decrease in ϵHf values between 900 and 500 Ma. Locally,

negative ϵHf values are observed from 850 Ma to 750 Ma. From 750 to 700 Ma, there is a subtle shift towards more positive values, followed by a plateau that shifts back towards more negative values throughout the end of the Cryogenian and Ediacaran periods (Figure 2b).

2.3 | Lu–Hf, O and U–Pb Record During the Neoproterozoic

To investigate erosional patterns and sedimentary recycling into subduction zones, we calculated a moving Theil–Sen regression slope (Theil 1992) of $\delta^{18}\text{O}$ and ϵHf through time from 900 to 500 Ma in 5 Myr intervals, using a rolling window to evaluate changes in the slope and correlation strength (Figure 3). A window width of 10 Myr was defined with a start and end time of 500 Ma and 900 Ma, respectively. On the $\epsilon\text{Hf}/\delta^{18}\text{O}$ slope plot (Figure 3a), negative values imply ancient sediment-derived contributions, whereas positive values imply melting of more juvenile sources. The Spearman's Rank coefficient (R_s) plot (Figure 3b) shows the strength of the linear relationship between these variables. Spearman's coefficient ranges from 0 to 1 and 0 to -1 , indicating positive or negative correlations, respectively. A value of coefficient R_s between 0.4 and 0.69 implies a moderate correlation (Fowler et al. 2013). The $\epsilon\text{Hf}/\delta^{18}\text{O}$ slope suggests two major troughs at 875 Ma and at 690 Ma (Figure 3a), both with moderate correlations based on Spearman's Rank coefficient (R_s). Minor troughs with a less pronounced signature in the $\epsilon\text{Hf}/\delta^{18}\text{O}$ slope are also observed at 790 Ma and 630 Ma; however, the R_s value implies a weaker correlation (Figure 3b). Nevertheless, the timing of this latter step coincides within error with the timing of the Marinoan glaciation.

Crustal residence (CR) ages, defined by the difference between $\text{Hf } T_{\text{DM}^2}$ model age and the U–Pb crystallisation age for individual zircons, are used to characterise the duration a magma may have resided within the lithosphere (Hawkesworth et al. 2019). We applied LOESS to identify possible shifts through time in CR ages (Figure 3c). From 900 to 785 Ma, CR ages progressively increase, indicating a greater proportion of recycled ancient crust, with an exception between 785 Ma and 752 Ma, where a trough at 765 Ma evidences juvenile input. Between 752 Ma and 705 Ma, there is an obvious decrease in CR ages, suggesting a significant input of juvenile material spanning the onset of Sturtian glaciation. Subsequently, CR ages gradually increase from 705 Ma to 585 Ma, indicating ancient-crustal input. At 585 Ma to 535 Ma, a similar—but less pronounced—decrease occurs.

3 | Discussion

According to previous studies, various mechanisms can drive erosion, including tectonic events (e.g., Sobolev and Brown 2019) and/or glacial processes (e.g., Keller et al. 2019). However, the relationship between widespread glacial events, tectonic, LIP-related processes and erosional patterns is still debated. Several authors have proposed that the onset of the Snowball Earth could be related to the weathering of the fresh basaltic surface, consuming atmospheric CO_2 and triggering global cooling (Godd ris et al. 2003; Cox et al. 2016; Ernst et al. 2021; Pu et al. 2022).

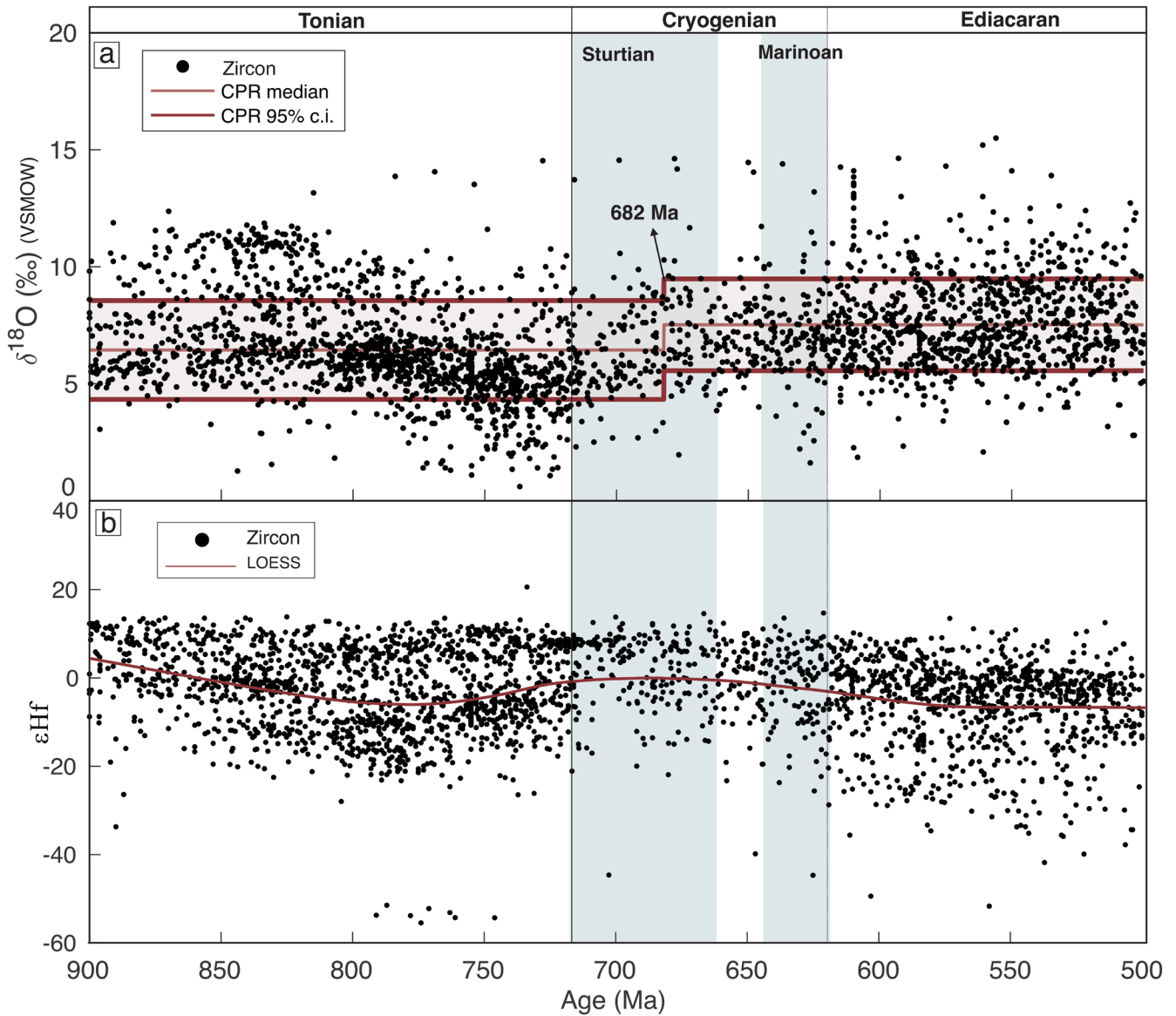


FIGURE 2 | Plot showing global zircon $\delta^{18}\text{O}$ values during the Neoproterozoic Era. A step-change is demonstrated by a Conjugate Partitioned Recursion (CPR) algorithm, showing an increase in $\delta^{18}\text{O}$ values at 682 Ma in data compiled from different regions (see Table S1 and Data S1). (b) Locally Estimated Scatterplot Smoothing (LOESS) applied to ϵ_{Hf} values through time. [Colour figure can be viewed at [wileyonlinelibrary.com](https://onlinelibrary.wiley.com)]

The Cryogenian glaciation occurred during a period of pronounced tectonic instability associated with the breakup of the supercontinent Rodinia (Hoffman et al. 2017). An intrinsic connection between tectonic activity, erosive forces, and recycling of sediments into magmatic systems is feasible. For example, Spencer et al. (2022) proposed that crustal reworking increased during supercontinent assembly based on zircon U–Pb and $\delta^{18}\text{O}$. Eyles and Janaszczak (2004) proposed a zipper-rift model suggesting a link between the length of Rodinia's rifted margins, climatic impacts of elevated rift margins, and consequent sediments deposited in surrounding rift basins. Enhanced continental erosion may ultimately lead to increased sediment volumes delivered to subduction trenches (Sobolev and Brown 2019).

Although glaciers are commonly associated with locally high rates of erosion (Wilner et al. 2024), the Snowball Earth glaciations were originally suggested to have been associated with a limited hydrological cycle and less erosive ice sheets (Hoffman

and Schrag 2002). However, various observations would appear to counter this idea, suggesting dynamic ice masses and an active hydrological cycle during this period (Ali et al. 2018; Condon et al. 2002; le Heron et al. 2011). The sedimentology of Sturtian deposits, therefore, appears to support a more dynamic glaciation at least at these low latitudes.

Here, using the zircon $\epsilon_{\text{Hf}}/\delta^{18}\text{O}$ slope, we show important changes associated with the recycling of sediments into magmatic systems that may provide additional insights into significant changes from the Tonian to Ediacaran periods.

3.1 | Late Tonian to Cryogenian

Zircon ϵ_{Hf} and $\delta^{18}\text{O}$ data presented in this study suggest two state changes. In Figure 3a, the $\epsilon_{\text{Hf}}/\delta^{18}\text{O}$ slope shows two abrupt decreases at 875 Ma and 690 Ma (Figure 3a). The oldest shift at

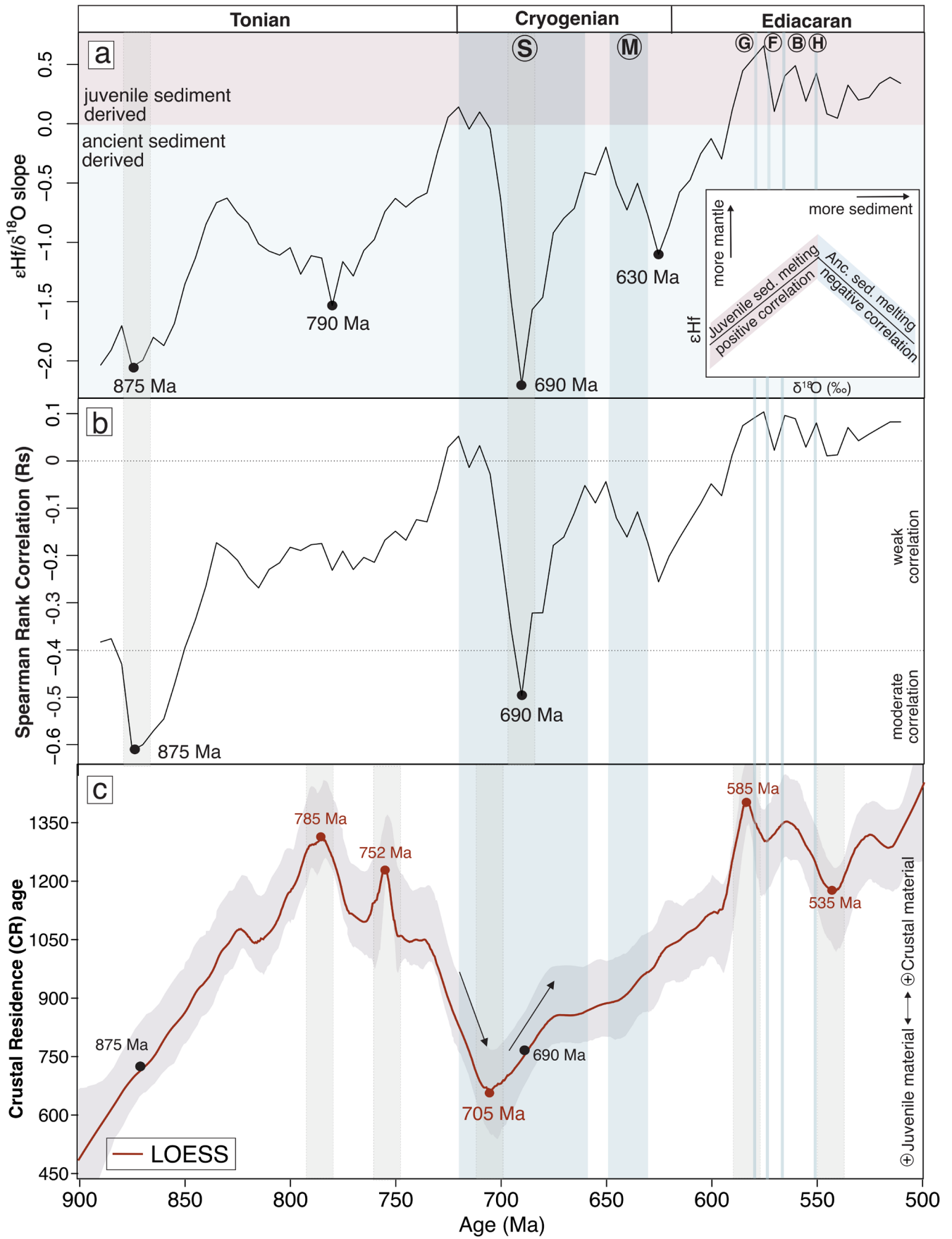


FIGURE 3 | Legend on next page.

FIGURE 3 | Statistical relationship between ϵ_{Hf} and $\delta^{18}\text{O}$ of zircon during the Sturtian (S) and Marinoan (M) glaciations. Ediacaran glacial episodes were also included: (G) Gaskiers; (F) Fauquier; (B) Bou-Azzer; (H) Hankalchough. (a) Slope line of the Theil Sen regression line for $\epsilon_{\text{Hf}}/\delta^{18}\text{O}$ through time. Two major peaks are observed at 875 Ma and 690 Ma. Idealised diagram shows ϵ_{Hf} and $\delta^{18}\text{O}$ plot, where negative values represent ancient sediment-derived contributions and positive values are related to the melting of juvenile sediments. (b) Spearman Rank correlation between ϵ_{Hf} and $\delta^{18}\text{O}$ through time (note that the moving window used is 20 Myr at 5 Myr intervals). (c) LOESS Crustal Residence (CR) curve versus U–Pb age—a significant decrease in crustal ages occurs between ca. 750 Ma and 705 Ma, preceding the Sturtian glaciation. This data corroborates with previous studies suggesting that the extensive LIP emplacement could potentially trigger increased weatherability and erosion, leading to glacial events. [Colour figure can be viewed at [wileyonlinelibrary.com](https://onlinelibrary.wiley.com)]

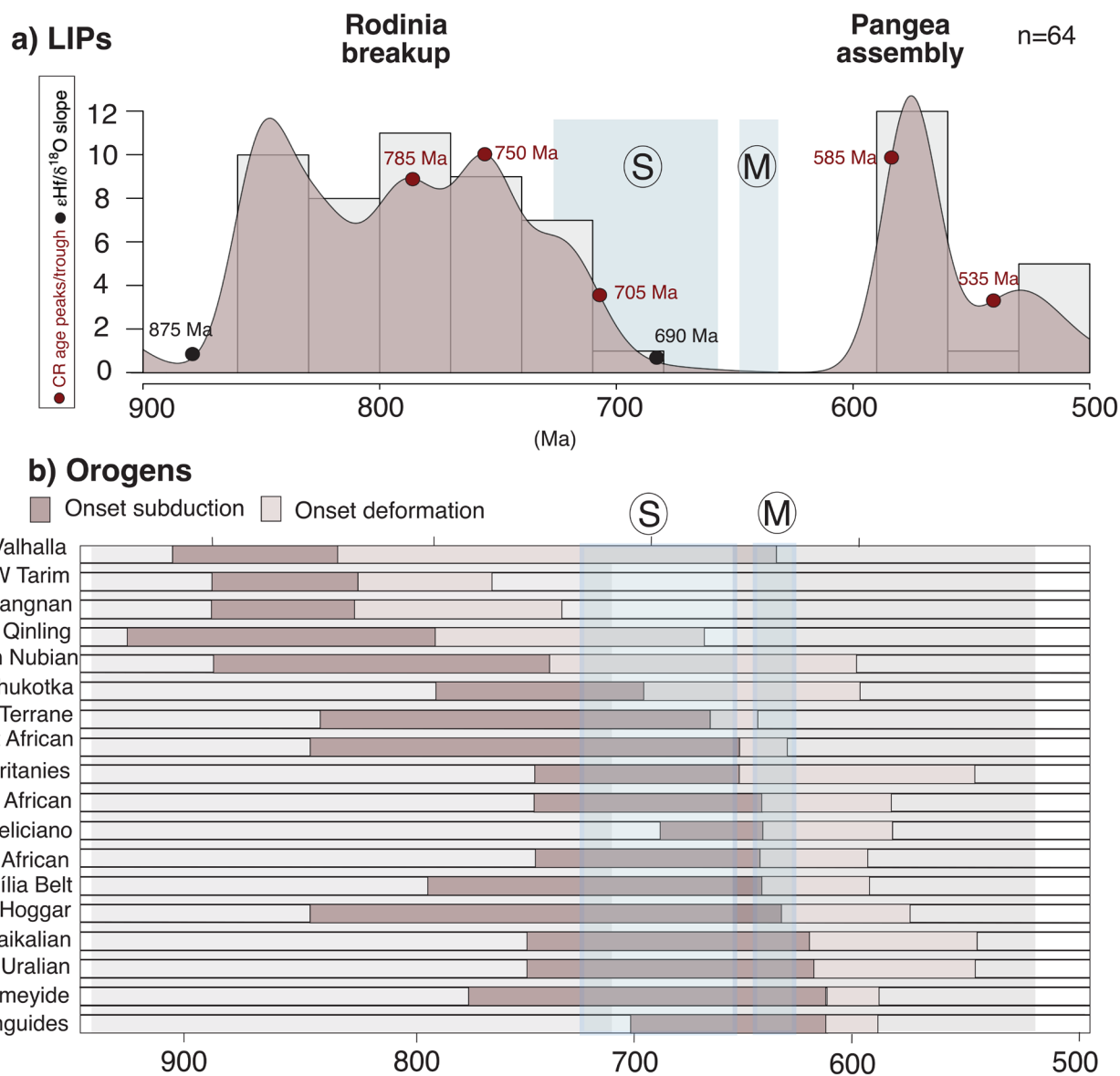


FIGURE 4 | (a) Global LIP frequency diagram from 900 Ma to 500 Ma based on previous work (Ernst et al. 2021). There is a significant decrease of LIP occurrence preceding the glacial episodes, although important LIP events are associated with the Sturtian glaciation (e.g., Franklin LIP). The main shifts evidenced by both $\epsilon_{\text{Hf}}/\delta^{18}\text{O}$ (black) and CR (red) plots are highlighted by the circles. (b) The frequency of orogens over the studied interval using the compilation (Condie et al. 2022) shows that the Sturtian glaciation coincides with the onset of subduction in different regions, which might trigger tectonic instability and uplift, while the Marinoan glacial event coincides mostly with the transition between the final subduction onset and the onset of deformation. [Colour figure can be viewed at [wileyonlinelibrary.com](https://onlinelibrary.wiley.com)]

875 Ma is consistent with the LOESS fit through crustal residence times, which indicates an increase of older input between 900 and 785 Ma. The late Mesoproterozoic to early Tonian period is marked by accretionary events linked to the assembly of the

Rodinia supercontinent, with the earliest record of subduction at 1000–950 Ma and younger subduction zones around 760 Ma (Figure 4). This was followed by widespread continental rifting and the breakup of Rodinia (Cawood et al. 2016). Therefore, we

propose that the 875Ma trough ($\epsilon_{\text{Hf}}/\delta^{18}\text{O}$ slope) mostly reflects the melting of ancient sedimentary material due to collision, exhumation, and subsequent erosional processes during the final stages of Rodinia's assembly.

The LOESS curve applied to CR ages reveals a significant trough at 765Ma between two prominent crustal input peaks at 785 Ma

and 752Ma. This pattern could be related to the emplacement of multiple plumes at 780Ma (Godd ris et al. 2003), leading to a greater availability of juvenile material to be eroded and delivered into marine environments, ultimately recycled into magmatic systems via subduction. A 752Ma crustal peak is followed by a drastic increase of juvenile material persisting until 705 Ma, that temporally overlaps with the emplacement of the

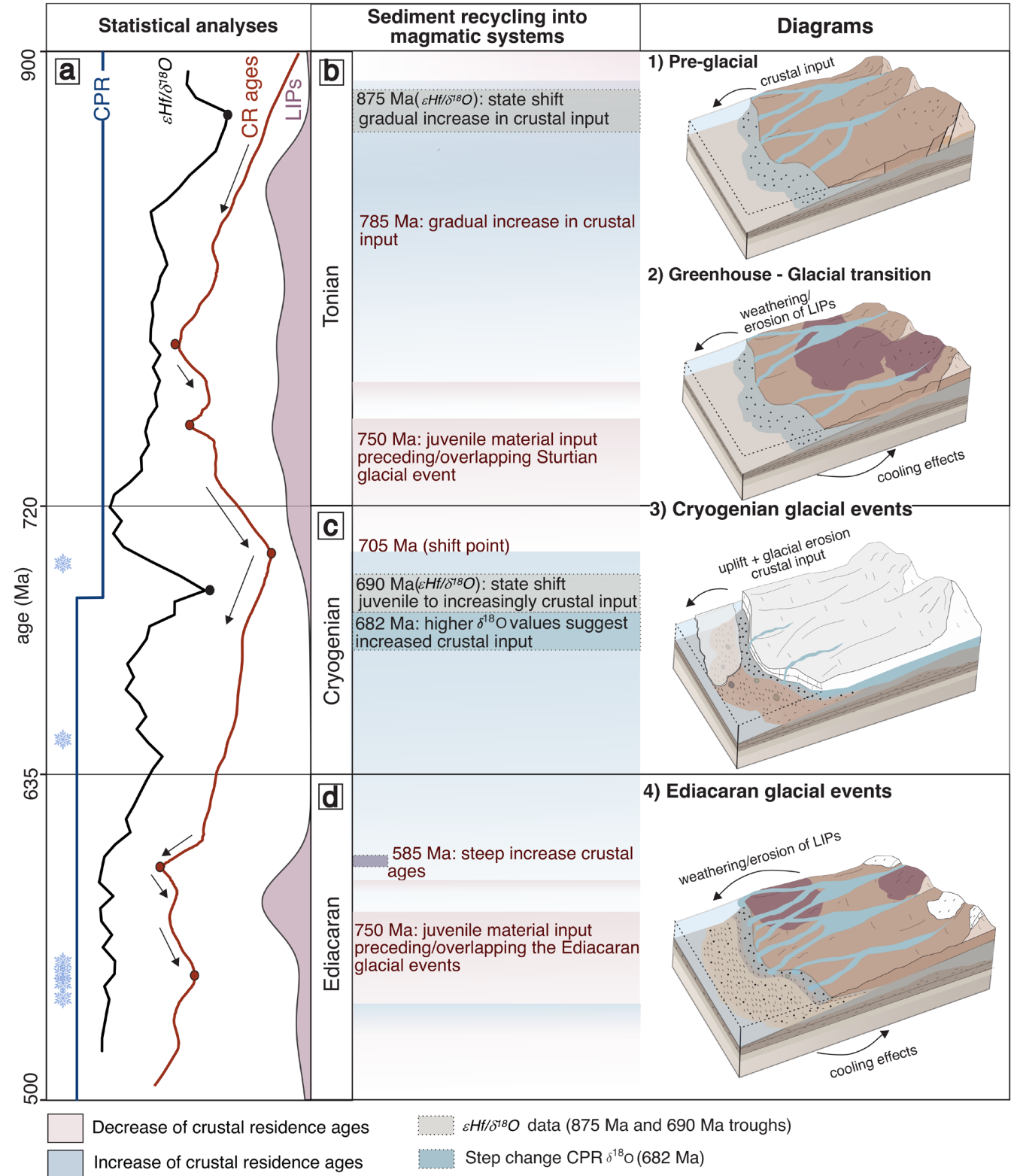


FIGURE 5 | Legend on next page.

FIGURE 5 | (a) Statistical methods are combined with LIP histogram to visualise possible relationship between different processes through time—CPR at $\delta^{18}\text{O}$ values through time (blue), $\epsilon\text{Hf}/\delta^{18}\text{O}$ Spearman correlation (black), Crustal Residence (CR) ages (red). (a) The $\epsilon\text{Hf}/\delta^{18}\text{O}$ slope correlation tracks the transition from juvenile to increasingly crustal input, as evidenced by the pre-glacial Tonian showing a shift in $\epsilon\text{Hf}/\delta^{18}\text{O}$ slope at ca. 875 Ma. The 875 Ma trough is associated with orogenic processes tied to Rodinia's final assembly and intense LIP emplacement, with sediment being transported mostly by fluvial and aeolian processes, ultimately leading to recycling of crustal sediment into subduction zones. This is followed by an increase of juvenile material input preceding/partially overlapping the onset of Sturtian glaciation (ca. 750 Ma and 705 Ma), at the Tonian-Cryogenian boundary. (b) This is followed by an increase in older crustal input starting at 705 Ma, reinforced by a shift in $\epsilon\text{Hf}/\delta^{18}\text{O}$ slope at ~690 Ma and a shift in the $\delta^{18}\text{O}$ values at ~682 Ma, which is interpreted as a response to tectonic and glacial erosion. (c) A similar— but less pronounced— pattern is recognised preceding and during the Ediacaran glacial events, where intense LIP activity is accompanied by an increase of crustal-input, immediately followed by an increase of juvenile material (585–535 Ma). [Colour figure can be viewed at [wileyonlinelibrary.com](https://onlinelibrary.wiley.com)]

ca. 725–712 Ma Franklin LIP (northern Laurentia) and with the onset of the Sturtian glaciation, and preceded by the emplacement of global LIP events at ca. 755 Ma (Ernst et al. 2021). According to several authors, the combination of LIP emplacement, incipient rifting of Rodinia, and intense tropical weathering could trigger a snowball state (Cox et al. 2016; Donnadieu et al. 2004; Godd ris et al. 2003). Horton (2015) suggested higher carbonate ^{13}C values as a response to increased fluvial phosphorus transfer into ocean basins via this weathering. The dataset we investigate corroborates these interpretations, indicating increasing erosional rates of juvenile material preceding and partially overlapping the Sturtian glacial episode.

From 705 Ma to 585 Ma, a gradual increase in CR ages coincides with both the timing of a 690 Ma pulse revealed by the $\epsilon\text{Hf}/\delta^{18}\text{O}$ slope and a step change to higher $\delta^{18}\text{O}$ values, consistent with an increase of sediment into magmatic systems. The Sturtian glaciation occurs simultaneously with the initiation of subduction in different regions (Figures 4 and 5), which might have led to tectonic instability and increasing erosion. A notable coincident shift in the sedimentary provenance of circum-Rodinian basins during the Sturtian was also considered to be caused by intensified erosion during frigid periods (e.g., Rugen Elias et al. 2024; Kirkland et al. 2025). The dynamic and complex nature of glacial environments, marked by advances and retreats of ice, likely contributed to exposure of ancient basement and glaciogenic erosion to some degree. Therefore, we hypothesise that the gradual shift towards more crustal input into magmatic systems was driven by a combination of both glacial and tectonic processes.

The Marinoan glacial interval shows a less pronounced trough in the $\epsilon\text{Hf}/\delta^{18}\text{O}$ plot, while a gradual increase in crustal input is implied by generally increasing crustal residence time. There is no LIP event currently described between the Sturtian and the Marinoan episodes (Ernst et al. 2021), and tectonic events are mostly related to later stages of subduction processes (Figure 4). Previous studies have suggested a causal relationship between the Pan-African orogenesis and the Marinoan event (Godd ris et al. 2007).

3.2 | Ediacaran Glacial Events

A subtle similarity is recognised when comparing the temporal emplacement of LIPs and the crustal residence age pattern from the Sturtian glacial event and the younger Ediacaran glacial episodes. The Ediacaran period is marked by the emplacement

of LIPs spanning 570 to 580 Ma (Ernst et al. 2021), followed by four glacial episodes, including the Gaskiers (580 Ma), Fauquier (571 Ma), Bou-Azzer (566 Ma) and Hankalchough (551 Ma) (Retallack 2022). G mez et al. (2025) suggest rapid sediment recycling and broader sediment sourcing during the Gaskiers deglaciation. Based on the LOESS fit to CR ages, a period of LIP emplacement appears immediately followed by two subtle periods of increased juvenile material recycling into subduction zones, spanning the onset of glacial events (Figures 3 and 5).

4 | Conclusions

A global compilation of zircon U–Pb–Hf–O isotopes identifies two major transitions from mantle-derived to increasingly crustal input at ca. 875 Ma and ca. 690 Ma, conceivably linked to distinct geodynamic and climatic processes also at this time. The Tonian $\epsilon\text{Hf}/\delta^{18}\text{O}$ trough reflects enhanced sediment recycling during Rodinia's final assembly, primarily driven by tectonics. In contrast, the Cryogenian signal records a strong increase in juvenile recycling preceding and during glacial onset. Both $\epsilon\text{Hf}/\delta^{18}\text{O}$ and CR state shifts imply a transition from juvenile material to ancient sediment input at 705–682 Ma, possibly driven by orogen-related sediment delivery and glacial erosion during the Sturtian glaciation. These results highlight the complexity and interconnected nature of deep, shallow, surface, and atmospheric processes, suggesting a causal link between LIP emplacement, global cooling, and increased crustal input during frigid conditions. These results must be tempered with known geological challenges of a temporally incomplete record with spatial bias. Additional ϵHf and $\delta^{18}\text{O}$ data from unrepresented regions may help shed further light on these important processes.

Acknowledgements

The authors also acknowledge the two anonymous reviewers for their significant contribution to this manuscript. T.M.G. and T.K.H. gratefully acknowledge support from the WoodNext Foundation, a donor-advised fund program.

[Correction added on 24 October 2025, after first online publication: An Acknowledgements section has been added at the request of the corresponding author.]

Disclosure

GitHub code available https://github.com/marinaseraine-cyber/cryogenian_glaciation.

Conflicts of Interest

The authors declare no conflicts of interest.

Data Availability Statement

The data that supports the findings of this study are available in the Supporting Information—S1 of this article.

References

- Ali, D. O., A. M. Spencer, I. J. Fairchild, et al. 2018. “Indicators of Relative Completeness of the Glacial Record of the Port Askaig Formation, Garvellach Islands, Scotland.” *Precambrian Research* 319: 65–78.
- Allen, P. A., and J. L. Etienne. 2008. “Sedimentary Challenge to Snowball Earth.” *Nature Geoscience* 1: 817–825.
- Bindeman, I. 2008. “Oxygen Isotopes in Mantle and Crustal Magmas as Revealed by Single Crystal Analysis.” *Reviews in Mineralogy and Geochemistry* 69: 445–478. <https://doi.org/10.2138/rmg.2008.69.12>.
- Cawood, P. A., R. A. Strachan, S. A. Pisarevsky, D. P. Gladkochub, and J. B. Murphy. 2016. “Linking Collisional and Accretionary Orogens During Rodinia Assembly and Breakup: Implications for Models of Supercontinent Cycles.” *Earth and Planetary Science Letters* 449: 118–126. <https://doi.org/10.1016/j.epsl.2016.05.049>.
- Christie-Blick, N., L. E. Sohl, and M. J. Kennedy. 1999. “Considering a Neoproterozoic Snowball Earth.” *Science* 284: 1087. <https://doi.org/10.1126/science.284.5417.1087a>.
- Condie, K. C., S. A. Pisarevsky, S. J. Puetz, C. J. Spencer, W. Teixeira, and F. Meira Faleiros. 2022. “A Reappraisal of the Global Tectono-Magmatic Lull at ~2.3 ga.” *Precambrian Research* 376: 106690. <https://doi.org/10.1016/j.precamres.2022.106690>.
- Condon, D., A. R. Prave, and D. Benn. 2002. “Neoproterozoic Glacial-Rainout Intervals: Observations and Implications.” *Geology* 30: 35–38.
- Cox, G. M., G. P. Halverson, R. K. Stevenson, et al. 2016. “Continental Flood Basalt Weathering as a Trigger for Neoproterozoic Snowball Earth.” *Earth and Planetary Science Letters* 446: 89–99. <https://doi.org/10.1016/j.epsl.2016.04.016>.
- Donnadieu, Y., Y. Godd eris, G. Ramstein, A. N ed elec, and J. Meert. 2004. “A ‘Snowball Earth’ Climate Triggered by Continental Break-Up Through Changes in Runoff.” *Nature* 428: 303–306. <https://doi.org/10.1038/nature02408>.
- Eriksson, P. G., S. Banerjee, O. Catuneanu, et al. 2013. “Secular Changes in Sedimentation Systems and Sequence Stratigraphy.” *Gondwana Research* 24: 468–489. <https://doi.org/10.1016/j.gr.2012.09.008>.
- Ernst, R. E., D. P. G. Bond, S. Zhang, et al. 2021. “Large Igneous Province Record Through Time and Implications for Secular Environmental Changes and Geological Time-Scale Boundaries.” *Large Igneous Provinces*: 1–26. <https://doi.org/10.1002/9781119507444.ch1>.
- Eyles, N., and N. Januszczak. 2004. “‘Zipper-Rift’: A Tectonic Model for Neoproterozoic Glaciations During the Breakup of Rodinia After 750 ma.” *Earth-Science Reviews* 65: 1–73. [https://doi.org/10.1016/S0012-8252\(03\)00080-1](https://doi.org/10.1016/S0012-8252(03)00080-1).
- Flowers, R. M., F. A. Macdonald, C. S. Siddoway, and R. Havranek. 2020. “Diachronous Development of Great Unconformities Before Neoproterozoic Snowball Earth.” *Proceedings of the National Academy of Sciences* 117: 10172–10180. <https://doi.org/10.1073/pnas.1913131117>.
- Fowler, J., L. Cohen, and P. Jarvis. 2013. *Practical Statistics for Field Biology*. John Wiley & Sons.
- Godd eris, Y., Y. Donnadieu, C. Dessert, et al. 2007. “Coupled Modeling of Global Carbon Cycle and Climate in the Neoproterozoic: Links Between Rodinia Breakup and Major Glaciations.” *Comptes Rendus G eoscience* 339: 212–222.
- Godd eris, Y., Y. Donnadieu, A. N ed elec, et al. 2003. “The Sturtian ‘Snowball’ Glaciation: Fire and Ice.” *Earth and Planetary Science Letters* 211: 1–12. [https://doi.org/10.1016/S0012-821X\(03\)00197-3](https://doi.org/10.1016/S0012-821X(03)00197-3).
- G omez, N., D. Lowe, A. Mills, S. Kommescher, and R. Lam. 2025. “Interplay of Ediacaran Glaciation and Sediment Provenance Revealed by Detrital Zircon U-Pb Geochronology and Hf Isotope Geochemistry in the Bonavista Peninsula (Newfoundland).” *Geological Society of America Bulletin*. <https://doi.org/10.1130/b38347.1>.
- Hawkesworth, C., P. A. Cawood, and B. Dhuime. 2019. “Rates of Generation and Growth of the Continental Crust.” *Geoscience Frontiers* 10: 165–173.
- Hoffman, P. F., D. S. Abbot, Y. Ashkenazy, et al. 2017. “Snowball Earth Climate Dynamics and Cryogenian Geology-Geobiology.” *Science Advances* 3: e1600983. <https://doi.org/10.1126/sciadv.1600983>.
- Hoffman, P. F., and D. P. Schrag. 2002. “The Snowball Earth Hypothesis: Testing the Limits of Global Change.” *Terra Nova* 14: 129–155.
- Horton, F. 2015. “Did Phosphorus Derived From the Weathering of Large Igneous Provinces Fertilize the Neoproterozoic Ocean?” *Geochemistry, Geophysics, Geosystems* 16: 1723–1738. <https://doi.org/10.1002/2015GC005792>.
- Keller, C. B., J. M. Husson, R. N. Mitchell, et al. 2019. “Neoproterozoic Glacial Origin of the Great Unconformity.” *Proceedings of the National Academy of Sciences* 116: 1136–1145. <https://doi.org/10.1073/pnas.1804350116>.
- Kirkland, C., R. Strachan, D. Archibald, and J. Murphy. 2025. “The Neoproterozoic Glacial Broom.” *Geology* 53: 435–440.
- Kirschvink, J. L. 1992. “Late Proterozoic Low-Latitude Global Glaciation: The Snowball Earth.” *Proterozoic Biosphere* 52: 51–52.
- le Heron, D. P., G. Cox, A. Trundle, and A. Collins. 2011. “Sea Ice-Free Conditions During the Sturtian Glaciation (Early Cryogenian), South Australia.” *Geology* 39: 31–34. <https://doi.org/10.1130/G31547.1>.
- Li, Z.-X., Y. Liu, and R. Ernst. 2023. “A Dynamic 2000–540 ma Earth History: From Cratonic Amalgamation to the Age of Supercontinent Cycle.” *Earth-Science Reviews* 238: 104336. <https://doi.org/10.1016/j.earscirev.2023.104336>.
- McDannell, K. T., C. B. Keller, W. R. Guenther, P. K. Zeitler, and D. L. Shuster. 2022. “Thermochronologic Constraints on the Origin of the Great Unconformity.” *Proceedings of the National Academy of Sciences of the United States of America* 119: e2118682119. <https://doi.org/10.1073/pnas.2118682119>.
- Mitchell, R. N., T. M. Gernon, A. Nordsvan, G. M. Cox, Z.-X. Li, and P. F. Hoffman. 2019. “Hit or Miss: Glacial Incisions of Snowball Earth.” *Terra Nova* 31: 381–389. <https://doi.org/10.1111/ter.12400>.
- Partin, C. A., and P. M. Sadler. 2016. “Slow Net Sediment Accumulation Sets Snowball Earth Apart From All Younger Glacial Episodes.” *Geology* 44: 1019–1022. <https://doi.org/10.1130/G38350.1>.
- Plank, T., K. A. Kelley, R. W. Murray, and L. Q. Stern. 2007. “Chemical Composition of Sediments Subducting at the Izu-Bonin Trench.” *Geochemistry, Geophysics, Geosystems* 8, no. 4. <https://doi.org/10.1029/2006gc001444>.
- Prave, A. R., D. J. Condon, K. H. Hoffmann, S. Tapster, and A. E. Fallick. 2016. “Duration and Nature of the End-Cryogenian (Marinoan) Glaciation.” *Geology* 44: 631–634. <https://doi.org/10.1130/G38089.1>.
- Pu, J. P., F. A. Macdonald, M. D. Schmitz, et al. 2022. “Emplacement of the Franklin Large Igneous Province and Initiation of the Sturtian Snowball Earth.” *Science Advances* 8, no. 47. <https://doi.org/10.1126/sciadv.adc9430>.
- Puetz, S. J., C. J. Spencer, K. C. Condie, and N. M. Roberts. 2024. “Enhanced U-Pb Detrital Zircon, Lu-Hf Zircon, $\delta^{18}\text{O}$ Zircon, and Sm-Nd Whole Rock Global Databases.” *Scientific Data* 11: 56.

- Retallack, G. J. 2022. “Towards a Glacial Subdivision of the Ediacaran Period, With an Example of the Boston Bay Group, Massachusetts.” *Australian Journal of Earth Sciences* 69: 223–250. <https://doi.org/10.1080/08120099.2021.1954088>.
- Rooney, A. D., C. Yang, D. J. Condon, M. Zhu, and F. A. Macdonald. 2020. “U-Pb and re-Os Geochronology Tracks Stratigraphic Condensation in the Sturtian Snowball Earth Aftermath.” *Geology* 48: 625–629. <https://doi.org/10.1130/G47246.1>.
- Rugen Elias, J., G. Pastore, P. Vermeesch, et al. 2024. “Glacially Influenced Provenance and Sturtian Affinity Revealed by Detrital Zircon U–pb Ages From Sandstones in the Port Askaig Formation, Dalradian Supergroup.” *Journal of the Geological Society* 181: jgs2024-029. <https://doi.org/10.1144/jgs2024-029>.
- Shields-Zhou, G., and L. Och. 2011. “The Case for a Neoproterozoic Oxygenation Event: Geochemical Evidence and Biological Consequences.” *GSA Today* 21: 4–11.
- Sobolev, S. V., and M. Brown. 2019. “Surface Erosion Events Controlled the Evolution of Plate Tectonics on Earth.” *Nature* 570: 52–57. <https://doi.org/10.1038/s41586-019-1258-4>.
- Spencer, C. J., N. S. Davies, T. M. Gernon, et al. 2022. “Composition of Continental Crust Altered by the Emergence of Land Plants.” *Nature Geoscience* 15: 735–740. <https://doi.org/10.1038/s41561-022-00995-2>.
- Theil, H. 1992. “A Rank-Invariant Method of Linear and Polynomial Regression Analysis.” In *Henri Theil's Contributions to Economics and Econometrics: Econometric Theory and Methodology*, edited by B. Raj and J. Koerts, 345–381. Springer Netherlands. https://doi.org/10.1007/978-94-011-2546-8_20.
- Valley, J., J. Lackey, A. Cavosie, et al. 2005. “4.4 Billion Years of Crustal Maturation: Oxygen Isotope Ratios of Magmatic Zircon.” *Contributions to Mineralogy and Petrology* 150: 561–580.
- Wang, R., Z. Yin, and B. Shen. 2023. “A Late Ediacaran Ice Age: The Key Node in the Earth System Evolution.” *Earth-Science Reviews* 247: 104610. <https://doi.org/10.1016/j.earscirev.2023.104610>.
- Wilner, J. A., B. J. Nordin, A. Getraer, et al. 2024. “Limits to Timescale Dependence in Erosion Rates: Quantifying Glacial and Fluvial Erosion Across Timescales.” *Science Advances* 10: eadr2009. <https://doi.org/10.1126/sciadv.adr2009>.

Supporting Information

Additional supporting information can be found online in the Supporting Information section. **Table S1:** ter70016-sup-0001-TableS1.xlsx. **Figure S1:** Distribution of ϵ_{Hf} and $\delta^{18}\text{O}$ data for Cryogenian samples, dated between 720 Ma and 635 Ma (compiled dataset from Puetz et al. 2024). **Figure S2:** Distribution of ϵ_{Hf} and $\delta^{18}\text{O}$ data for samples dated between 500 Ma and 900 Ma (compiled dataset from Puetz et al. 2024). **Data S1:** ter70016-sup-0004-Supinfo1.docx.